Hydraulic modeling of three flumes for minimal sedimentation

Juan Gabriel Brigido-Morales[1]

Mauricio Carrillo-García[1,§]

Jorge Víctor Prado-Hernández[1,2]

Jorge Flores-Velázquez[3]

1 Posgrado de Ingeniería Agrícola y Uso Integral del Agua-Universidad Autónoma Chapingo. Carretera México-Texcoco km 38.5, Chapingo, Texcoco, Estado de México, México. CP. 56230. (jgabriel.brigido@gmail.com).

2 Departamento de Suelos-Universidad Autónoma Chapingo. Carretera México-Texcoco km 38.5, Chapingo, Texcoco, Estado de México, México. CP. 56230. (jpradoh@chapingo.mx).

3 Postgrado en Hidrociencias, Campus Montecillo-Colegio de Postgraduados. Carretera México-Texcoco km 36.5. Montecillo, Texcoco, Estado de México, México. CP. 56230. (jorgelv@colpos.mx).

Autor para correspondencia: mauricio@correo.chapingo.mx.

Abstract

The sustainability of water use in agriculture is very important, and to achieve this, proper management of surface water resources is required, which, in small basins, depends on good measurement of flow rate data. This work analyzes the hydraulic performance of three proposed modified long-throated flumes with a 10% slope supercritical channel by using the WinFlume® v.1.06 software for a maximum flow of 50 L s^{-1}, for clean water and in conditions in which the cross section of the inlet was modified by sediments. Hydraulic simulations were performed for triangular, rectangular, and trapezoidal cross sections in the throat and the supercritical channel by using the Iber® v.2.5.2 software to compare the pattern of the WinFlume® gauging curve with the results of Iber®; the difference between both gauging curves was a maximum error of 3% in the three cross-sectional areas. For hydraulic simulation in the supercritical modified cross-sectional area for clean flow water and sediment flow water, data located at half the total length of the supercritical channel were taken. Variations in flow depth assuming sedimentation were negligible, and it was found that the water profile in the supercritical channel was not affected, so it can be used as an indicator. In addition, it was observed that the best cross-sectional area for the channel was the rectangular one with a maximum of 0.9997 R^2 for the flow rate curve (Q-h).

Keywords:

hydraulic simulation, natural runoff, sediment flow, water measurement.

Introduction

Mexico is a country of great territorial area (1 959 million km^2), which lacks the capacity to monitor its water resources since it only has 815 hydrometric stations operating (CONAGUA, 2019), located in the main rivers and strategic sites for the development of the country. Therefore, it is urgent to find alternatives to improve knowledge about the quantity, quality, and temporality of water available in the country.

Considering that, in developing countries such as Mexico, approximately 76% of the available water is used for irrigation (CONAGUA, 2019), its monitoring becomes more relevant, especially for sustainable management. Since, as pointed out by De Fraiture *et al.* (2010) in relation to the agricultural sector, some poorly conceived or implemented interventions have caused high social and environmental costs, such as inequitable allocation of water and adverse impacts on ecosystems.

Given the need to quantify water, the use of gauging structures that allow reliable knowledge of the available volumes becomes relevant. At present, there is a great variety of flumes, where the most used are the weirs, which can be broad-crested or sharp-crested (WMO, 2010); in addition, their measurement section can be rectangular, triangular, or semicircular (Ibrahim, 2015; Haghshenas and Imanian *et al.*, 2021; Vatankhah, 2021). Other widely used structures are long-throated flumes, which are constructed for a wide variety of shapes and are generally very accurate when operated under non-submerged flow conditions (Clemmens *et al.*, 2001).

In all cases, the structures work well with clean water flow; however, in natural surface runoff, there is sediment entrainment (Prado *et al.*, 2017) and a frequent problem is their accumulation in the place where the water level is measured, to the point that the measurements lose validity (Castro-Orgaz and Mateos, 2014).

Given this situation, Carrillo (1999) suggested, as a possible solution to prevent errors caused by sedimentation, the addition of a rapid to a long-throated flume and finding a site with an adequate correlation between the depth of flow and the circulating flow rate; this alternative could be viable since it has been found that velocities greater than 0.25 m s^{-1} are sufficient to promote sediment entrainment and thus prevent sedimentation (Ackers *et al.*, 2001; Blokker *et al.*, 2011).

Therefore, this work presented an initial advance that considered the hydraulic analysis through numerical simulations of three different geometries for long-throated flumes, to which a rapid was added after the throat with a 10% slope and the elevation of the bottom of the structure was modified.

Materials and methods

Design of gauging structures

Three long-throated flumes were designed with the WinFlume$^{®}$ v.1.06 software, selecting different geometries for the control section (throat): rectangular, trapezoidal, and triangular. In all cases, an operating range from 10 to 50 L s^{-1} and material with absolute roughness ks of 0.00006 m were proposed; in addition, the flow rate gauging table of each structure was obtained, measured with flow depth increments of 1 cm (17 flow rates). A rapid was added to each designed structure and two scenarios were generated to study the effects of sediment accumulation on the gauging structures.

Scenario 1: Geometry of the designed flume

Table 1 shows the dimensions of the structures designed, including the quick proposal for their study. In the convergence section, only the length is indicated since their width, depth and side slopes coincide upstream with the inlet channel and downstream with the control section (Figure 1).

Table 1. Dimensions of the gauging structures designed.

		Rectangular flume	Trapezoidal flume	Triangular flume
Inlet channel (section I)	Length (m)	0.5	0.7	0.5
	Base width (m)	0.4	0.25	0.24
	Depth (m)	0.4	0.32	0.44
	Side slopes (m)	0:1	0.5:1	0.5:1
Convergence (section II)	Length (m)	0.3	0.2	0.44
Throat or control section (section III))	Elev. on inlet channel (m)	0.05	0.05	0.1
	Length (m)	0.35	0.2	0.44
	Base width (m)	0.25	0.15	-
	Depth (m)	0.35	0.27	0.34
	Side slopes (m)	0:1	0.5:1	0.8:1
Rapid (section IV)	Horizontal length (m)	0.5	0.5	0.5
	Slope (%)	10	10	10

Figure 1. Isometric view of the designed flumes: a) rectangular flume; b) trapezoidal flume; and c) triangular flume.
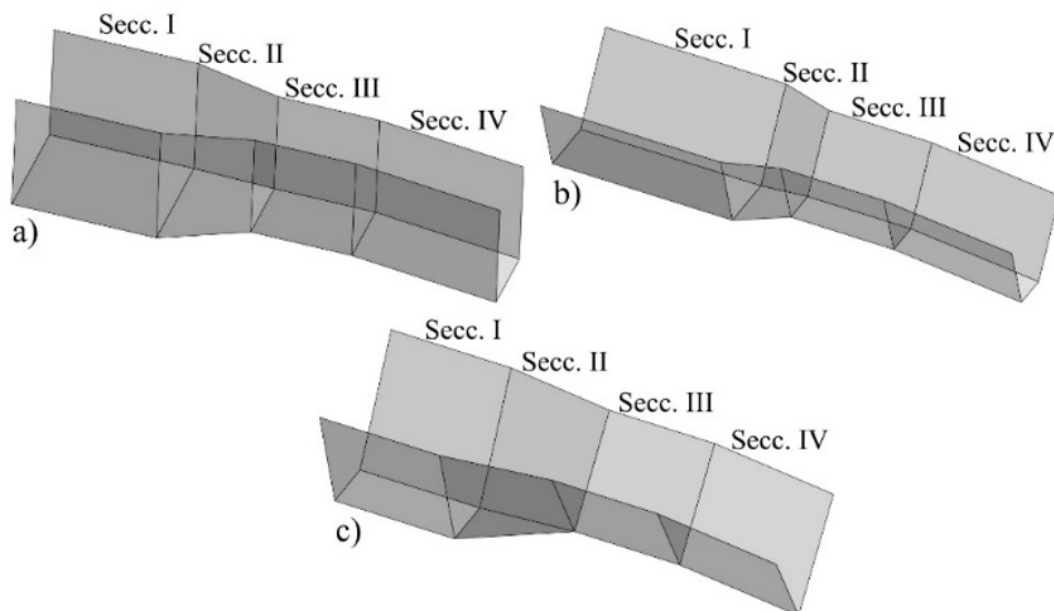

Scenario 2: Scenario 1 + modification to the inlet

To test sedimentation effects on the development of the flow in the rapid, the elevation of the bottom of the inlet channel and convergence section of each flume was modified until reaching the elevation of the control section, generating structures with new dimensions of width and depth (Table 2 and Figure 2).

Table 2. Dimensions of gauging structures designed to test the effect of sediment accumulation at the inlet of the structure.

		Rectangular flume	Trapezoidal flume	Triangular flume
Inlet channel (section I)	Length (m)	0.5	0.7	0.5
	Base width (m)	0.4	0.3	0.34
	Depth (m)	0.35	0.27	0.34
	Side slopes (m)	0:1	0.5:1	0.5:1
Convergence (section II)	Length (m)	0.3	0.2	0.44
Throat or control section (section III)	Length (m)	0.35	0.2	0.44
	Base width (m)	0.25	0.15	-
	Depth (m)	0.35	0.27	0.34
	Side slopes (m)	0:1	0.5:1	0.8:1
Rapid (section IV)	Horizontal length (m)	0.5	0.5	0.5
	Slope (%)	10	10	10

Figure 2. Isometric view of the designed flumes, with modifications in the inlet and convergence sections: a) rectangular flume; b) trapezoidal flume; and c) triangular flume.
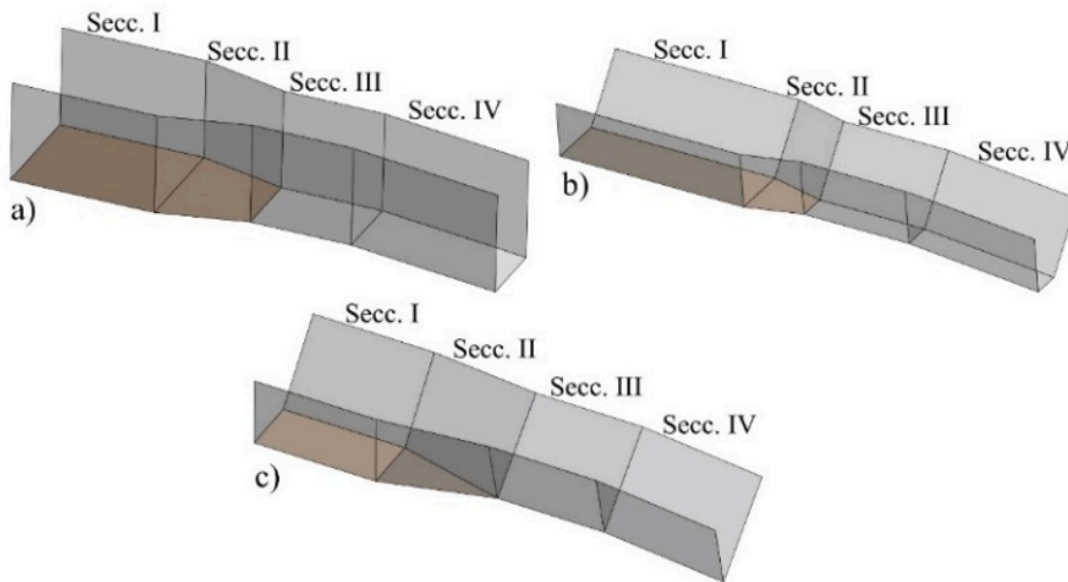
Determination of roughness values (n) for proposed gauging structures

From the data of the gauging table, a value of the Manning roughness coefficient was calculated for the results of each expense obtained, considering the hydraulic characteristics of the inlet of the structure (hydraulic area, wet perimeter, hydraulic diameter), relative roughness and Reynolds number, using an equation derived from the Manning and Darcy-Weisbach equations (equation 1) and the Colebrook equation (equation 2);

$$n=\frac{1}{\sqrt{8g}}R_h^{\frac{1}{6}}\sqrt{f} \quad (1) \quad .\frac{1}{\sqrt{f}}=-2\log_{10}\left(\frac{k/D}{3.7}+\frac{2.51}{Re\sqrt{f}}\right)$$

2).

Where:n is the Manning roughness coefficient (dimensionless); g is the acceleration of gravity ($m\cdot s^{-2}$); R_h is the hydraulic radius (m); f is the Darcy friction factor (dimensionless); k is the absolute roughness (m);D is the hydraulic diameter (m); and Re is the Reynolds number (dimensionless). An average value for the Manning coefficients was then calculated, obtaining a value of 0.0121 for the rectangular flume, 0.0123 for the trapezoidal flume and 0.0133 for the triangular flume.

Numerical simulation of water flow in the flumes

The simulation of the water flow in the gauging structures was carried out using the Iber® v.2.5.2 program, which solves the Saint Venant two-dimensional equations, incorporating the effects of turbulence and surface friction by wind through equations 3, 4 and 5 (Bladé *et al.*, 2014):

$$\frac{\partial h}{\partial t}+\frac{\partial hU_x}{\partial x}+\frac{\partial hU_y}{\partial y}=0$$

3).

$$\frac{\partial h}{\partial t}\frac{\partial hU_x}{\partial x}\frac{\partial hU_y}{\partial y}\quad\frac{\partial}{\partial t}(hU_x)+\frac{\partial}{\partial x}\left(hU_x^2+g\frac{h^2}{2}\right)+\frac{\partial}{\partial y}(hU_xU_y)=-gh\frac{\partial Z_b}{\partial x}+\frac{\tau_{s,x}}{\rho}-\frac{\tau_{b,x}}{\rho}+\frac{\partial}{\partial x}\left(v_th\frac{\partial U_x}{\partial x}\right)+\frac{\partial}{\partial y}\left(v_th\frac{\partial U_x}{\partial y}\right)$$

4).

$$\frac{\partial}{\partial t}(hU_y)+\frac{\partial}{\partial y}\left(hU_y^2+g\frac{h^2}{2}\right)+\frac{\partial}{\partial x}(hU_xU_y)=-gh\frac{\partial Z_b}{\partial y}+\frac{\tau_{s,y}}{\rho}-\frac{\tau_{b,y}}{\rho}+\frac{\partial}{\partial x}\left(v_th\frac{\partial U_y}{\partial x}\right)+\frac{\partial}{\partial y}\left(v_th\frac{\partial U_y}{\partial y}\right)$$

5).

Where: h is the depth (m);U_x and U_y are the horizontal velocities averaged in depth in the main and transverse direction to the flow ($m\ s^{-1}$);g is the acceleration of gravity ($m\ s^{-2}$); g is the density of water;Z_b is the height of the bottom; т s is the friction on the free surface due to friction produced by the wind; τ_s is the friction due to bottom friction; and v_t is turbulent viscosity.

The geometric models for scenarios 1 and 2 were configured, defining the Manning roughness coefficients for the walls as obtained: 0.0121 for the rectangular flume, 0.0123 for the trapezoidal and 0.0133 for the triangular flume, except the lower part of the inlet and convergence sections of the proposed flumes of scenario 2, in which case a coefficient of 0.023 was used, considering the characteristics of the deposited material (Chow, 1988).

In all cases, a numerical discretization was performed based on a structured mesh consisting of elements of 0.5 cm × 1 cm, placing the largest side along the structure (predominance of flow). The imposed boundary conditions were constant flow rate in subcritical regime at the inlet of the flumes and flow in critical/supercritical regime at the outlet.

The k-# turbulence model of Rastogi and Rodi was used since it is one of the most recurrent for shallow turbulent flows and with good results obtained through experimentation (Cea et al., 2007; Bladé et al., 2014). The simulation for the case of each flume was carried out in permanent regime for each flow rate, with the aim of obtaining the best precision of the gauging tables of the designed structures (scenarios 1 and 2); a total of 132 simulations were performed.

Determination of flow depth and processing of results

The depth of flow in the inlet section was determined according to the requirements specified for each design (Clemmens et al., 2001), the determination sites were located 0.3 m, 0.5 m, and 0.32 m upstream of the beginning of the convergence in the rectangular, trapezoidal, and triangular flumes, respectively. The site selected in the rapids was located in all cases at half its length.

In addition, at each site, five readings were made in a direction transversal to the flow and an average value was obtained.

Evaluation of the performance of numerical simulations

To evaluate the performance of the numerical simulation carried out in Iber$^®$ with respect to the flow at the inlet of the flumes, the values of flow depth were measured to be compared with those obtained with WinFlume$^®$, three statistical indicators were used: scatter index (SI), mean absolute percentage error (MAPE) and the root mean square error (RMSE), expressed mathematically in equations 6, 7 and 8 (Yousif et al., 2019).

$$SI=\frac{\sqrt{\frac{\sum_{i=1}^{N}(\varphi_{i\text{-calc}}-\varphi_{i\text{-sim}})^2}{N}}}{\overline{\varphi_{i\text{-calc}}}}\times100$$

6).

$$MAPE=\frac{100}{N}\sum_{i=1}^{N}\frac{|\varphi_{i\text{-calc}}-\varphi_{i\text{-sim}}|}{\phi_{i\text{-calc}}}$$

7).

$$RMSE=\sqrt{\frac{\sum_{i=1}^{N}(\varphi_{i\text{-calc}}-\varphi_{i\text{-sim}})^2}{N}}$$

8).

Where: $\varphi_{i\text{-calc}}$ is the flow depth value (cm) obtained in the design with WinFlume; $\varphi_{i\text{-sim}}$ is the i-th value obtained for the flow depth (cm) in the hydraulic simulation with Iber; N is the number of data analyzed; and $\varphi_{i\text{-calc}}$ is the average of the flow depth values (cm) obtained with WinFlume.

Obtaining flow rate-flow depth (Q-h) functional relationships at the inlet and rapid of the flumes

With the data from the gauging table obtained with WinFlume and the measurements made in the rapid, the Q-h curves of each flume (both scenarios) were plotted and the data were fitted to an equation characteristic of weirs, which is usually expressed in the form (Saul, 1997):$Q= k\cdot h^n$ 9). Where Q is the flow rate (L s^{-1}); h is the depth of flow (cm); and k and n are constants (dimensionless). In addition, the coefficient of determination (R^2) was calculated, which represents the percentage of variability in the dependent variable; that is, the variance with respect to the mean (Chicco et al., 2021).

## Determination of flow variation in the rapid for scenarios 1 and 2

To verify the reliability of the measurements made in the rapid, despite the modifications made in the inlet of the structures, using the same indicators shown in equations 6, 7 and 8, the variation between the data measured in the rapids of the structures proposed in scenario 1 and the data measured in the rapids of the structures included in scenario 2 was evaluated.

Results and discussion

Relationship between flow rates and flow depth for designed flumes

Based on the original design of the gauging structures, with the data of the gauging tables obtained from each structure Figure 3 shows the behavior of the depth of the water, in the inlet section of the flumes, corresponding to the circulating flow rates.


Figure 3. Relationship between flow rates and depth at the inlet.
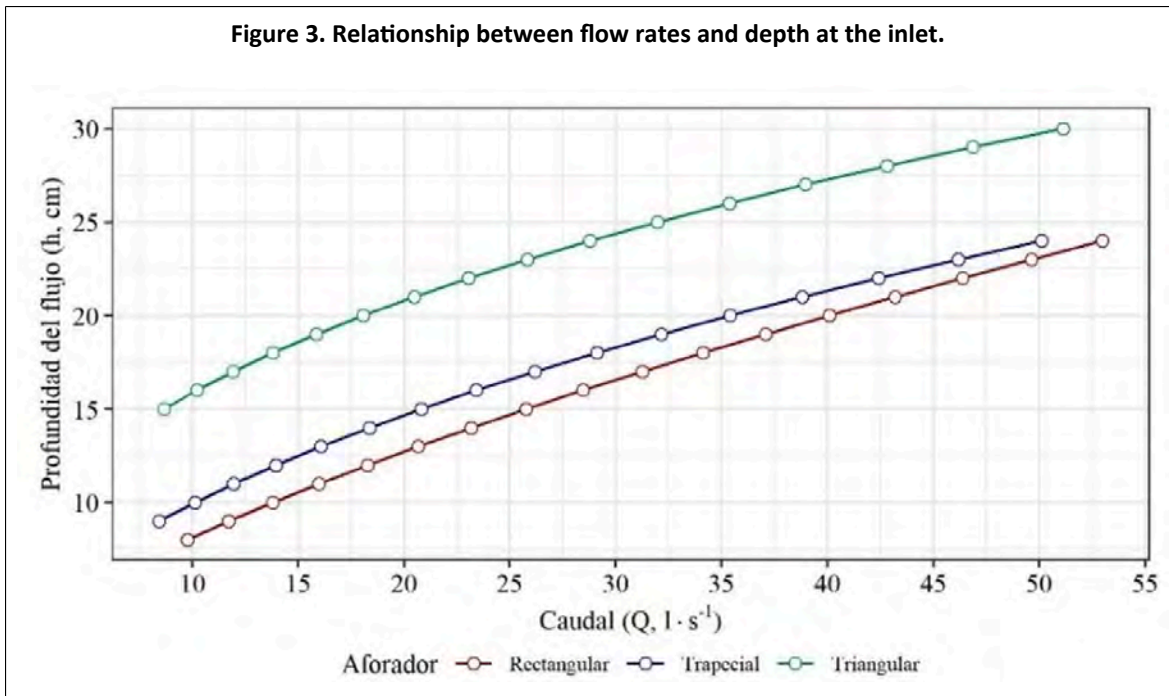
Behavior of the flow obtained from the numerical simulation

Regarding the hydraulic simulations performed with Iber®Figure 4 shows the results obtained, particularly the results for flow depth in the rectangular flume, although in this case the total depth is shown, while the value reported in WinFlume® is referenced to the bottom of the throat; that is, the result must be subtracted 5 cm.

Figure 4. **Flow behavior in the rectangular flume corresponding to scenario 1, for a flow rate of 25.7666 L s⁻¹.**
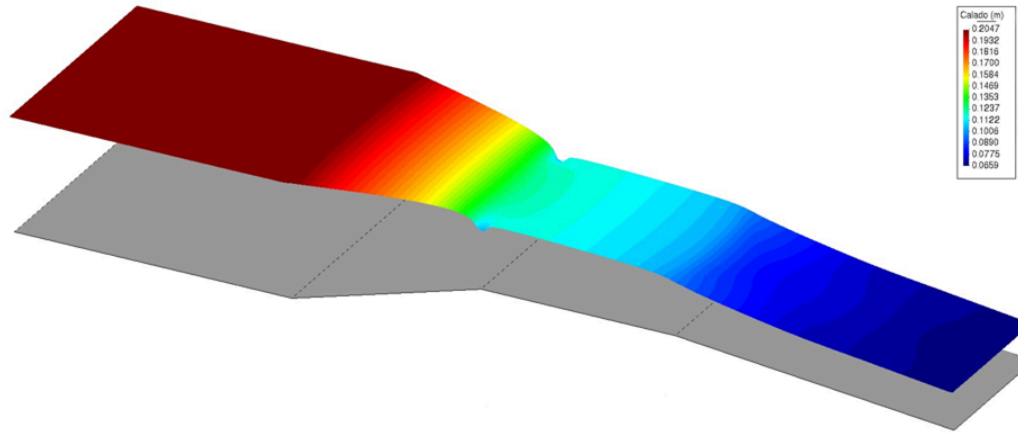
When processing the information, it was obtained that the values of the depth of flow at the inlet of the structures were slightly higher compared to those obtained with WinFlume®; however, the difference was constant for the entire range of flow rates, the results can be observed in Table 3.

Table 3. Estimated values of the depth of flow obtained with Iber®.

Rectangular flume		Trapezoidal flume		Triangular flume	
Q (L s⁻¹)	H (cm)	Q (L s⁻¹)	H (cm)	Q (L s⁻¹)	H (cm)
9.7656	8.18				
11.7155	9.21	8.4277	9.18	8.6664	15.2
13.7855	10.24	10.1158	10.2	10.2186	16.2
15.9693	11.27	11.9512	11.21	11.9295	17.21
18.2624	12.31	13.9359	12.26	13.8051	18.22
20.6637	13.35	16.0718	13.26	15.8513	19.22
23.1666	14.39	18.3591	14.32	18.0739	20.24
25.7666	15.44	20.8038	15.31	20.4759	21.24
28.4577	16.48	23.4064	16.37	23.0585	22.26
31.2422	17.52	26.1695	17.38	25.817	23.27
34.1196	18.57	29.0955	18.39	28.7926	24.31
37.0778	19.62	32.1602	19.41	31.9728	25.34
40.0957	20.67	35.4009	20.49	35.3634	26.29
43.1855	21.7	38.8187	21.53	38.9625	27.3
46.3736	22.74	42.4099	22.51	42.7911	28.3
49.6385	23.8	46.1753	23.48	46.8476	29.35
52.9784	24.84	50.1202	24.57	51.1377	30.33

Q= flow rate; h= flow depth.

Performance of numerical simulations

The results obtained with the simulations were used to obtain the statistical indicators shown in Table 4, where it can be seen that, in all cases, the error obtained was less than 3%, even in the case of the triangular flume the calculated error did not exceed 2%. These results support the reliability of the results obtained through numerical simulation since, if it is considered that the authors of WinFlume® indicate that the error supported analytically and experimentally in the designed flumes is approximately 2%, it can be inferred that in the worst case scenario, there would be an error of ±5% with respect to the true value.

Table 4. Statistical indicators for the h values of the prototype and model.

	Rectangular flume	Trapezoidal flume	Triangular flume
SI (%)	2.92	2.06	1.03
MAPE (%)	2.94	2.19	1.2
RMSE (cm)	0.468	0.329	0.232

Flow rate-flow depth (Q-h) curves at the inlet and rapid of the flumes

The data from the gauging tables obtained with WinFlume® for the structures included in scenario 1, in addition to the results obtained with the numerical simulations, were used to obtain fitted equations between the flow rate and flow depth at the inlet of the section (Table 5). A variation in the fitted equations is observed; however, in all cases, values very close to 1 were obtained for the coefficients of determination (R^2).

Table 5. Fitted equations and coefficient of determination at the inlet of the flumes.

| Software	Flume	Fitted equation	Coefficient of determination
WinFlume®	Rectangular flume	$Q= 0.4016 \cdot h^{1.5365}$	$R^2= 0.999996$
	Trapezoidal flume	$Q= 0.1394 \cdot h^{1.8498}$	$R^2= 0.999828$
	Triangular flume	$Q= 0.0083 \cdot h^{2.564}$	$R^2= 0.999996$
Iber®	Rectangular flume	$Q= 0.4043 \cdot h^{1.518}$	$R^2= 0.999997$
	Trapezoidal flume	$Q= 0.1361 \cdot h^{1.844}$	$R^2= 0.99976$
	Triangular flume	$Q= 0.0079 \cdot h^{2.57}$	$R^2= 0.999973$

Q= flow rate (L s-1); h= flow depth (cm).

It is possible to notice, according to the value of R^2, that the best fit for WinFlume® data is achieved with the triangular and rectangular flumes. However, the data obtained with Iber® indicate a better fit with the rectangular flume, followed by the triangular one and finally the trapezoidal one.

Figure 5 shows the Q-h relationships obtained in the rapids of the flumes when analyzing the results of the numerical simulations, where the cross of the curves of the trapezoidal and rectangular channels is explained by the greater rate of increase of the hydraulic area of a trapezoidal section with respect to a rectangular one when increasing its depth, in addition to the behavior of the supercritical regime that generates transverse waves resulting in the formation of the 'oblique jump'.

Figure 5. Fit of Q-h curves for measurements of the selected site in the rapid of the three flumes included in scenario 1.
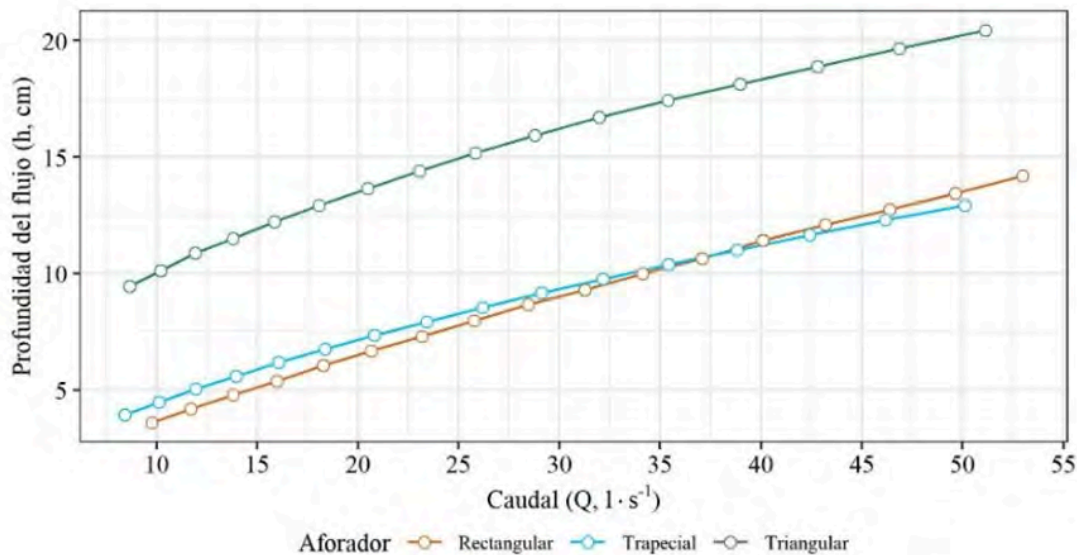
The equation models fitted to the data measured in the rapids of the structures belonging to scenario 1, together with their coefficient of determination (R^2), are shown in Table 6. Where, despite having a good fit in the three flumes, it can be noted again that the best fit is obtained with the rectangular section flume with an R^2 closer to 1.

Table 6. Fitted equations and coefficient of determination calculated from measurements at the selected site of the rapid gauging structures.

	Fitted equation	Coefficient of determination
Rectangular flume	$Q= 2.041\ h^{1.272}$	$R^2= 0.999995$
Trapezoidal flume	$Q= 0.921{\cdot}h^{1.5034}$	$R^2= 0.999414$
Triangular flume	$Q= 0.0513{\cdot}^{h2.2877}$	$R^2= 0.999925$

Flow variation in the rapid for scenarios 1 and 2

Regarding the variation between the results of the numerical simulations in the rapids of the flumes, for the analyzed scenarios, it was found that a reduction of the hydraulic area at the inlet of the flume does not have a relevant effect on the behavior of the flow developed in the rapid because, as can be seen in Table 7, in none of the cases was an error greater than 1% reached.

Table 7. Statistical indicators calculated for the flow depth values determined with Iber® in scenario 2 compared to scenario 1 values.

	Rectangular flume	Trapezoidal flume	Triangular flume
SI (%)	0.2	0.5	0.13
MAPE (%)	0.16	0.39	0.12
RMSE (cm)	0.016	0.04	0.019

This is because, although the structure is modified at the bottom by the accumulation of sediments, it still maintains the design of a flume with lateral constrictions, which, according to Bos and Wijbenga (1997), have already been used previously for the measurement of flow rates in channels with sediment transport; also recently, the work by Aali and Vatankhah (2023) reported an average error close to 2.2% in flow rate measurement using simple channels with a trapezoidal contraction.

In this work, it was also found that in the two scenarios, the Froude number in the inlet channel always remained below 0.4, which is a requirement to achieve uniform surfaces of the water surface. By maintaining the conditions upstream of the throat, the conditions of flow developed in the throat and the rapid are also maintained.

Based on Table 7, the results indicate that the performance of the rectangular and triangular structure is similar; however, it is necessary to consider other aspects, such as those observed by the following researchers, in order to select the type of geometry suitable for use in natural flow conditions.

The research by Agazadeh and Mohammadi (2013) on the conditions of the incipient movement speed of sediment particles in channels of triangular section showed that the section of the channel has a significant impact because the walls of the channel are very close at the bottom, the flow is very weak, so a higher speed is necessary to reach the incipient movement of the sediment.

On the other hand, Aksoy et al. (2017) conducted an experimental work analyzing the flow of water with sediments in channels of trapezoidal, rectangular, circular, U-shaped, and V-bottom sections, where they found that, for the same slope, the channels of rectangular sections provide the lowest incipient sediment deposition rate, while the V-bottom channel has the highest incipient sediment deposition rate.

In this same sense, Unal (2018) reported that rectangular channels have a higher efficiency in sediment transport since sediment particles begin to be deposited under a lower shear stress in the rectangular channel compared to non-rectangular channels. Therefore, considering the results of these studies, together with the results found in this work, the convenience of using rectangular sections was observed.

Since the problem in all flumes is sedimentation, the basis of this research was the proposal to measure the flow rates in the rapid added, where the results obtained show the development of velocities in a range from 0.5 to 2 m s^{-1}, being greater than those indicated by Ackers et al. (2001); Blokker et al. (2011) to promote sediment entrainment, the problem of sedimentation accumulation is prevented and consequently a constant reading of circulating flow rates is ensured.

Conclusions

Although variations were observed in the flow depths determined in Iber with respect to those originally obtained with WinFlume$^{®}$, the results showed a maximum error of ±5%. Derived from the analysis between scenarios 1 and 2, it was found that the accumulation of sediments at the inlet of the structure has a minimal effect on the development of flow conditions because in none of the simulated flow rates was a Froude number higher than 0.4 found, this condition allows the structure to continue working correctly and consequently that the variations in the depth of the flow in the rapid are less to 1%.

Based on the results of simulations and reviews of other experimental studies that have shown that the presence of bottom sediments in the flow is a reason to consider in more detail the selection of the type of flume to install, it was concluded that a flume with rectangular geometry is more suitable for its construction and flow rate conditions in natural channels.

It is recommended to carry out more detailed research to achieve the best performance of the selected structure, proposing other slopes for the rapids and also other measurement sites in

them; all this aimed at determining the characteristics of a structure that could offer the best alternative for its implementation in the field, which includes its experimental study.

Bibliography

1   Aali, F. and Vatankhah, A. R. 2023. Experimental study of simple flumes with trapezoidal contraction. Flow measurement and instrumentation. 90:102328. Doi: 10.1016/j.flowmeasinst.2023.102328.

2   Ackers, J.; Brandt, M. and Powell, J. 2001. Hydraulic characterization of deposits and review of sediment modelling. UK water industry research, London, UK. 01/DW/03/18.

3   Agazadeh, B. and Mohammadi, M. 2013. Experimental study of incipient motion of non-cohesive sediment in a rigid triangular channel. *In*: 16th International conference on transport & sedimentation of solid particles. Rostock University, Rostock, Germany. 1-8 pp.

4   Aksoy, H.; Safari, M. J. S.; Unal, N. E. and Mohammadi, M. 2017. Velocity based analysis of sediment incipient deposition in rigid boundary open channels. Water Science and Technology. 76(9):2535-2543.

5   Bladé, E.; Cea, L.; Corestein, G.; Escolano, E.; Puertas, J.; Vázquez-Cendón, E.; Dolz, J. y Coll, A. 2014. Iber: herramienta de simulación numérica del flujo en ríos. Revista Internacional de Métodos Numéricos para Cálculo y Diseño en Ingeniería. 30(1):1-10.

6   Blokker, E. J. M.; Vreeburg, J. H. G.; Schaap, P. G. and van Dijk, J. C. 2011. The self-cleaning velocity in practice. Water Distribution Systems Analysis. 187-199 pp.

7   Bos, M. G. and Wijbenga, J. H. A. 1997. Passage of sediment through flumes and over weirs. Irrigation and Drainage Systems. 11:29-39. Doi: 10.1023/A:1005752711183.

8   Carrillo, G. M. 1999. Sediment-resistant flume for hydrologic measurements. Tesis doctoral. Universidad de Arizona. Repositorio Institucional Universidad de Arizona. 15-104 pp.

9   Castro-Orgaz, O. and Mateos, L. 2014. Water discharge measurement in agricultural catchments using critical depth flumes affected by sediment deposition. Journal of Irrigation Drainage Engineering. 140(3):04013018. Doi: 10.1061/(asce)ir.1943-4774.0000672

10 Cea, L.; Puertas, J. and Vázquez-Cendón, M. E. 2007. Depth averaged modelling of turbulent shallow water flow with wet-dry fronts. Archives of Computational Methods in Engineering. 14(3):303-341. Doi: 10.1007/s11831-007-9009-3.

11 Chicco, D.; Warrens, M. J. and Jurman, G. 2021. The coefficient of determination R-squared is more informative than SMAPE, MAE, MAPE, MSE and RMSE in regression analysis evaluation. PeerJ Computer Science. 7:e623.

12 Chow, Ven Te. 1988. Open channel hydraulics, McGraw-Hill book company. New York USA. 680 p.

13 Clemmens, A. J.; Wahl, T. L.; Bos, M. G. and Reploge, J. A. 2001. Water measurement with Flumes and Weirs. International Institute for Land reclamation and improvement (ILRI). Publication 58. Wageningen, The Netherlands. 382 p.

14 Comisión Nacional del Agua. 2019. Atlas de agua en México. Ed. Secretaría de Medio Ambiente y Recursos Naturales (SEMARNAT). Cd. Méx.

15 De Fraiture, C.; Molden, D. and Wichelns, D. 2010. Investing in water for food, ecosystems, and livelihoods: an overview of the comprehensive assessment of water management in agriculture. Agricultural Water Management. 97(4):495-501. Doi:10.1016/j.agwat.2009.08.015

16 Haghshenas, V. and Vatankhah, A. R. 2021. Discharge equation of semicircular side weirs: an experimental study. Flow measurement and instrumentation . 81:102041.

17   Ibrahim, M. M. 2015. Bed profile downstream compound sharp crested V notch weir. Alexandria Engineering Journal. 54(3):607-613.

18   Imanian, H.; Mohammadian, A. and Hoshyar, P. 2021. Experimental and numerical study of flow over a broad crested weir under different hydraulic head ratios. Flow measurement and instrumentation . 80:102004.

19   Prado-Hernández J. V.; Rivera-Ruíz, P.; León-Mojarro, B.; Carrillo-García, M. y Martínez-Ruíz, A. 2017. Calibración de los modelos de pérdidas de suelo USLE y MUSLE en una cuenca forestal de México: caso El Malacate. Agrociencia. 51(3):265-284.

20   Saul, A. J. 1997. Combined sewer overflows. *In*: Sewers: rehabilitation and new construction repair and renovation. Ed. 1 Butterworth Heinemann. Oxford, UK. 283-317 pp.

21   Unal, N. E. 2018. Shear stress-based analysis of sediment incipient deposition in rigid boundary open channels. Water. 10(10):1399.

22   Yousif, A. A.; Sulaiman, S. O.; Diop, L.; Ehteram, M.; Shahid, S.; Ansari, N. and Yaseen, Z. M. 2019. Open channel sluice gate scouring parameters prediction: different scenarios of dimensional and non-dimensional input parameters. Water . 11(2):353.

Hydraulic modeling of three flumes for minimal sedimentation